Neurology Perspectives xxx (2021) xxx–xxx

NEUROLOGY PERSPECTIVES

www.journals.elsevier.com/neurology-perspectives

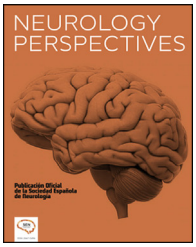

ORIGINAL ARTICLE

Ortho-coumaric acid derivatives with therapeutic potential in a three-dimensional culture of the immortalised U-138 MG glioblastoma multiforme cell line

Y.K. Gutiérrez Mercado[a], J.C. Mateos Díaz[b], D.D. Ojeda Hernández[b], F.J. López Gonzalez[c], E.E. Reza Zaldivar[d], M.A. Hernández Sapiens[d], U.A. Gómez Pinedo[e], R.S. Estrada[f], M. Macías Carballo[a], A.A. Canales Aguirre[d,*]

[a] *Laboratorio biotecnológico de Investigación y Diagnóstico, departamento de Clínicas, División de Ciencias Biomédicas, Centro Universitario de los Altos, Universidad de Guadalajara, Tepatitlán de Morelos, Jalisco, Mexico*
[b] *Unidad de Biotecnología Industrial del Centro de Investigación y Asistencia en Tecnología y Diseño del Estado de Jalisco A.C. (CIATEJ), Zapopan, Jalisco, Mexico*
[c] *Unidad de Neurocirugía, Hospital Civil, Fray Antonio Alcalde, Guadalajara, Mexico*
[d] *Unidad de Evaluación Preclínica, Biotecnología Médica y Farmacéutica, CONACYT Centro de Investigación y Asistencia en Tecnología y Diseño del Estado de Jalisco (CIATEJ), Guadalajara, Jalisco, Mexico*
[e] *Servicio de Neurología, Hospital Clínico San Carlos, IdiSSC, Facultad de Medicina, Universidad Complutense, Madrid, Spain*
[f] *Departamento de Neurocirugía, Facultad de Medicina y Ciencias. Clínica Mayo, Jacksonville, FL, United States*

Received 31 July 2021; accepted 15 September 2021
Available online xxxx

KEYWORDS
Glioblastoma multiforme;
3D studies;
Synthesis of ortho-coumaric acid alkyl esters;
Cytotoxicity;
Apoptosis;
Anticancer effect

Abstract
Introduction: The treatment of such primary brain tumours such as glioblastoma multiforme (GBM) presents numerous difficulties, considerably impacting patient survival rates. The search for new compounds with therapeutic potential focuses on the identification of molecules that can be produced through chemical and enzymatic processes and that present anticancer effects in different types of tumours.
Methods: Given the need for new treatments for GBM, we conducted a study to synthesise ortho-coumaric acid alkyl esters (OCAAE) and to evaluate them in an appropriate study model, a three-dimensional (3D) culture using the Matrigel extracellular matrix. We tested cytotoxicity with the 3-(4,5-dimethylthiazol-2-yl)-2,5-diphenyltetrazolium bromide (MTT) technique and by determining phosphatidylserine externalisation with annexin V and active caspase-3 expression as markers of apoptosis, and the subsequent degradation of DNA as a marker of cell death.

* Corresponding author at: Ave. Normalistas 800, Colinas de la Normal, Guadalajara, Jalisco C.P 44270, Mexico.
E-mail address: acanales@ciatej.mx (A.A. Canales Aguirre).

https://doi.org/10.1016/j.neurop.2021.09.006

Please cite this article as: Y.K. Gutiérrez Mercado, J.C. Mateos Díaz, D.D. Ojeda Hernández, et al., Ortho-coumaric acid derivatives with therapeutic potential in a three-dimensional culture of the immortalised U-138 MG glioblastoma multiforme cell line, Neurology Perspectives, https://doi.org/10.1016/j.neurop.2021.09.006

Results: Medium-chain OCAAEs, such as butyl-o-coumarate (BOC) and its isomer, showed the greatest effect on most of the parameters evaluated in 3D cultures of GBM, followed by methyl-, propyl-, and ethyl-o-coumarate (MOC, POC and EOC); these compounds showed effects both in reducing cell viability and in increasing the expression of active caspase-3 and annexin V and the degradation of DNA, in comparison with the first-line treatment for GBM, temozolomide.
Conclusion: These results, together with those of previous researchers, show that the different OCAAEs have a potential therapeutic effect on GBM, and that 3D culture of GBM cells is an appropriate model for the study of new antitumour molecules.

PALABRAS CLAVE
Glioblastoma multiforme;
Estudios en 3D;
Síntesis de alquil-ésteres del ácido orto-cumárico;
Citotoxicidad;
Apoptosis;
Efecto anticancerígeno

Resumen
Introducción: Los tumores cerebrales primarios como el Glioblastoma multiforme (GBM) presentan muchas dificultades para su tratamiento, lo que repercute considerablemente en la tasa de supervivencia del paciente. La búsqueda de nuevos compuestos con potencial terapéutico se enfoca en la identificación de moléculas, mismas que pueden ser producidas química y enzimáticamente; y que muestren efectos anticancerígenos en distintos tipos de tumores.
Metodología: La necesidad de nuevos tratamientos para el GBM, nos lleva a sintetizar alquil-ésteres del ácido orto-cumárico (ae-AOC) y a evaluarlos en un modelo de estudio apropiado como es el cultivo en tercera dimensión (3D) empleando la matriz extracelular, Matrigel™, mediante pruebas de citotoxicidad celular como el Bromuro de 3-(4,5-dimetiltiazol-2-il)-2,5-difenil tetrazolio (MTT), externalización de la fosfatidilserina, con Anexina V y la expresión de caspasa-3 activa como marcadores de apoptosis y la subsecuente degradación de ácido desoxirribonucleico (ADN) como marcador de muerte celular.
Resultados: Los ae-AOC de cadena mediana, como el butil-o-cumarato (BOC) y su isómero, presentaron un efecto significativo mayor en la mayoría de los parámetros evaluados en los cultivos en 3D de GBM, siguiendo de forma significativa el metil, el propil y el etil-o-cumarato (MOC, POC y EOC), presentaron efectos tanto en la reducción de la viabilidad celular como en el incremento en la expresión de caspasa-3 activa, Anexina V y la degradación del ADN, en comparación con el tratamiento de primera línea para los GBM, temozolomida (TMZ).
Conclusión: Estos resultados, aunados a investigaciones previas, muestran que los diferentes ae-AOC poseen un potencial efecto terapéutico, en los GBM, y que el cultivo de células de GBM en 3D es un modelo apropiado para el estudio de nuevas moléculas antitumorales.

Introduction

Glioblastoma multiforme (GBM) is one of the most relevant primary malignant brain tumours given its high mortality rate (90%); the mean survival time after diagnosis is no longer than 18 months, mainly due to the limited therapeutic options: not all chemotherapy agents cross the blood–brain barrier or cause resistance, surgical management is not always possible due to tumour location, and response to radiotherapy is poor.[1]

Brain tumours present an incidence rate of 23.79 cases per 100,000 person-years (7.08 for malignant tumours and 16.71 for benign tumours); GBM is the most frequent malignant tumour. In 2020, 24,970 cases of malignant tumours were recorded, and 81,246 patients died due to this type of tumour between 2013 and 2017.[1]

The first-line treatment for GBM is temozolomide (TMZ), an alkylating agent belonging to the imidazotetrazine class of drugs; as it presents a physiological pH, it is converted via hydrolysis to the active metabolite 3-methyl-(triazen-1-yl) imidazole-4-carboxamide, which acts through DNA methylation and acetylation to induce cell-cycle arrest of cancer cells.[2,3] However, many tumours are resistant to this drug, reducing patients' life expectancy. Thus, researchers have sought other molecules, including monoclonal antibodies, that may act as coadjuvant agents in the treatment of GBM.[4,5]

The search for new molecules for comprehensive treatment of GBM has focused on the following issues: 1) reducing drug resistance[6–8]; 2) inhibiting angiogenesis to prevent blood supply to the tumour[9,10]; 3) preventing progression, migration, and metastasis; and 4) promoting cell-cycle arrest or inducing apoptosis.[11–13]

Coumaric acid is a phenolic compound belonging to the class of hydroxycinnamic acids. It is usually found in three bioactive forms, according to the position of the hydroxyl group (-OH) in the aromatic ring: ortho-coumaric (if -OH is located at the second carbon [C2]), meta-coumaric (C3), or

para-coumaric acid (C4). The latter form has been studied most extensively due to its abundance in nature, whether free or bound to other molecules; these compounds are present in the roots, flowers, fruit, or seed of many plants.[14,15] Potentially useful derivatives of these acids can be obtained through chemical, enzymatic, or microbiological processes.[16–18] Coumaric acid and its derivatives present considerable antioxidant activity due to the hydroxyl groups on the phenolic ring. They also present anti-inflammatory, antiproliferative, proapoptotic, and antitumour properties, among others, depending on the compound under study, the method of extraction or synthesis, dose, and other factors affecting their biological activity.[19,20]

Ortho-coumaric acid (OCA) has attracted the least research attention; however, in cells from breast and colon cancers, melanomas, hepatocellular carcinomas, and other types of tumour, it is reported to activate such genes as *p53* and *Bax* and to increase the expression of proteins that promote caspase-dependent and caspase-independent apoptosis. It has also been observed to inhibit procarcinogenic genes, induce cell-cycle arrest, and inhibit matrix metalloproteinases 2 and 9, potentially conferring anticarcinogenic properties.[19–21] In this study, we evaluated the therapeutic potential of chemically synthesised OCA alkyl esters (OCAAE) as antitumour agents in a three-dimensional (3D) cell growth model using an extracellular matrix with GBM cells; this type of cell culture partially imitates the molecular, phenotypic, and cytohistological properties of the microenvironment present in brain gliomas *in vivo*.[22] This model represents a better experimental platform for cell characterisation and quantification of biomarkers, and serves as a pharmacological model, among other functions, and its results are comparable to the processes occurring *in vivo*. Therefore, these models enable preclinical studies to obtain more reliable results.[23,24]

Material and methods

Study design

In this study, we synthesised several OCAAEs (methyl-o-coumarate [MOC], ethyl-o-coumarate [EOC], propyl-o-coumarate [POC], butyl-o-coumarate [BOC], and isobutyl-o-coumarate [IOC]) and analysed their effect on the viability of GBM cells with different doses and exposure times, in monolayer and 3D cell cultures. We determined cell viability, externalisation of phosphatidylserine, expression of activated caspase-3, and DNA degradation; these procedures are described in greater detail below.

The outcome variables measured were the effect of alkyl chain elongation on the viability of GBM cells, the median lethal dose of each OCAAE, and the exposure time required for this effect to occur. We also determined which cell culture model best resembled the tumour environment for the analysis of the potential antitumour molecules under study.

GBM cell culture

The U-138 MG HTB-16 human GBM cell line was procured from American Type Culture Collection (ATCC; Rockville, USA) and cultivated in Dulbecco's Modified Eagle Medium (DMEM; Sigma-Aldrich, catalogue no. D6429) supplemented with 10% fetal bovine serum (Corning™, catalogue no. 35-016-CV) and 1% antibiotic-antimycotic (Gibco®, catalogue no. 15240062).

Cells were incubated at 37 °C and 5% CO_2; the medium was changed daily.

Three-dimensional cultures with Matrigel and monolayer culture

Matrigel base layer culture: Matrigel™ (Matrigel basement membrane matrix, catalogue no. 354234; Corning) was diluted at 50% with the culture medium and added to each well of a 96-well plate, then allowed to polymerise in an incubator at 37 °C for 15 min; we subsequently added cells diluted in the culture medium (5000 cells in 200 μL of medium in each well).

Matrigel-embedded cell culture: 5000 cells were diluted in 20 μL of medium and added to 20 μL of Matrigel (1:1 ratio), gently agitated without forming bubbles, and deposited in each well of a 96-well plate; the mixture was allowed to polymerise in an incubator at 37 °C for 15 min, then another 200 μL of medium was added.

Monolayer culture: 5000 cells diluted in 200 μL of medium were added to each well. All three cultures were incubated at 37 °C and 5% CO_2. We changed the medium and evaluated cell growth every day for 8 days.

On day 8, we repeated each culture, seeding three additional wells for each culture, with 5000 cells per well, as described above, and incubated for 6 h.

Subsequently, we tested the cell viability of each culture using the 3-(4,5-dimethylthiazol-2-yl)-2,5-diphenyltetrazolium bromide method (Sigma-Aldrich, Tox1, *in vitro* toxicology assay kit, MTT based), according to the manufacturer's instructions. MTT was converted to water-insoluble formazan crystals in viable cells; these were dissolved with dimethyl sulfoxide (DMSO) and studied at 570 nm in a microplate reader (Bio-Rad); the percentage of viable cells was calculated according to the following formula: optical density (treatment) × 100/optical density (control). After 8 days of growth, we compared the 3D and monolayer cultures, using the recently seeded monolayer wells (5000 cells per well) as the control condition.

Synthesis and purification of ortho-coumaric acid alkyl esters

The different types of OCAAE (MOC, EOC, POC, BOC, and IOC) were synthesised by Fischer esterification, using hydrogen chloride (HCl) as a catalyst.[26] Starting with 10% OCA dissolved homogeneously in the corresponding alcohol (ie, methanol, ethanol, propanol, butanol, or isobutanol), we added 5% HCl (at a concentration of 37%) and left the reaction in reflux for 12 to 24 h. Subsequently, the excess alcohol was evaporated in a Büchi rotavapor. The recovered oil was rinsed 3 times with 100 mL of a mixture of petroleum ether and ethyl ether 50% (*v*/*v*) to remove unreacted excess OCA.[27] The organic phase was recovered and the mixture of solvents removed with a Büchi rotavapor until we obtained a volume of approximately 6 mL of the sample, which was

loaded into a glass column (2 × 52 cm). Prior to this, the column was packed with 50 g of silica suspended in petroleum ether, with 0.5 g of quartz sand at the top. The alkyl ester was eluted with an increasing gradient of ethyl ether (0%–50% *v*/*v*) in petroleum ether. The output of the column was recovered in fractions of 8 mL using a Büchi vacuum pump. We used thin-layer chromatography (TLC) to analyse the fractions, and mixed only those containing the alkyl ester in question. Finally, the solvent was slowly evaporated in a fume hood to allow the reaction products to crystallise. The recovered crystals were stored at −20 °C in amber glass jars.[18]

Qualitative analysis by thin-layer chromatography

Qualitative analysis of the synthesis products and the fractions recovered was conducted on silica gel TLC plates with a fluorescent indicator (20 × 10 cm) (SIGMA; catalogue no. Z193291-1PAK); 5–10 μg of sample was manually injected 1 cm from the base of the plate. The different compounds were separated in a glass TLC chamber, which was previously equilibrated with a 2:1 (*v*/*v*) mixture of hexane and ethyl acetate. Excess solvent was evaporated in a fume hood and bands were viewed at 254 nm with a UVP handheld ultraviolet lamp.[18]

Working concentrations of study molecules

The molecules studied were: MOC, EOC, POC, BOC, IOC, and TMZ (Sigma-Aldrich, catalogue no. PHR1437-1G), used as the positive control; these molecules were diluted to the following working concentrations: 50 μM, 100 μM, 200 μM, 300 μM, 500 μM, and 1200 μM.

Evaluation of cell viability

GBM U-138-MG cells were seeded on a 96-well plate according to the monolayer and 3D Matrigel base layer culture, with 5000 cells per well; cultures were incubated for 3 days at 37 °C and 5% CO_2. On day 3, we removed the culture medium and added the working dilutions of OCAAEs, TMZ, vehicle (DMSO), and culture medium (control condition), in triplicate. Cultures were subsequently incubated for 24 h at 37 °C and 5% CO_2. After 24 h' exposure to the study molecules, we tested cell viability with the MTT technique described above.

We also conducted other experiments using only the 3D Matrigel base layer culture, using the same culture conditions, molecules, and dilutions, but with incubation periods of 24 h, 12 h, 6 h, and 3 h. After this period, the MTT assay was conducted.

Effect of combining ortho-coumaric acid alkyl esters and temozolomide

We repeated the cell viability study described above, except the 3D cultures of GBM cells were incubated for 24 h with each study molecule (BOC, IOC, MOC, POC, or EOC; 200, 300, or 500 μM) combined with 600 μM of TMZ on one plate, and with 1200 μM of TMZ on another plate. The MTT procedure was conducted after incubation.

Induction of apoptotic cell death secondary to ortho-coumaric acid alkyl esters

Detection of phosphatidylserine externalisation secondary to ortho-coumaric acid alkyl esters

This test used the monolayer culture of GBM cells at a density of 200,000 cells per well on a 24-well plate in triplicate. After 24 h' incubation, the medium was removed and the study molecules were added at the following concentrations: MOC, POC, and EOC at 300 μM; BOC at 200 μM; and TMZ at 600 μM. Cultures were incubated with the study molecules for 3 and 6 h. After incubation, the study molecules were removed and plates were washed with EDTA (2 mM) according to the annexin V protocol (Alexa Fluor 488 annexin V conjugate; Invitrogen, catalogue no. 3201 PHN1010 and PHN1008). Samples were studied by flow cytometry at 533 nm and 575 nm (Guava easyCyte 5, Millipore).

Caspase-3 activation

The 3D Matrigel base layer culture was cultured in an 8-well chamber slide (Thermo-Scientific, catalogue no. 154461-PK, Nunc Lab-Tek™ II Chamber Slide System) at a density of 20,000 cells per well; cultures were incubated for 72 h in culture medium at 37 °C and 5% CO_2. Subsequently, we added the following molecules: BOC at 200 μM; MOC, POC, and EOC at 300 μM; and TMZ at 600 μM. Cultures were incubated for 6 h, 12 h, and 24 h. After incubation, we removed the culture medium with the study molecules and added 4% paraformaldehyde in phosphate buffer solution (0.1 M, pH 7.4) for 2 h. For the immunofluorescence study, anti–caspase-3 antibodies (Abcam; ab13847 cysteine-protease-3) were added at a dilution of 1:500; the mixture was incubated overnight at 4 °C. The Alexa Fluor 488 secondary antibody (1:500, Vector Laboratories) was added and the mixture was stored in the dark for 2 h, protected with a drop of mounting medium with 4′,6-diamidino-2-phenylindole dihydrochloride (Fluoroshield, Abcam; ab104139); samples were analysed under a fluorescence microscope (Leica DM4 DF7000T; Leica Biosystems, Wetzlar, Germany). Analysis was conducted with the Leica Application Suite (LAS) X software (version 3.1.1.15751; Leica Biosystems) and images were acquired with a 40× objective and a Leica DFC7000T camera (Leica Biosystems). We ensured that the intensity of fluorescence was the same for each image acquisition and each group. For each image, we counted the total number of cells (DAPI) and caspase-3–labelled cells (green) in 10 fields (1.5 mm^2) in each well (3 wells) for each group, and calculated the percentage of labelled cells, following a double-blinded methodology.

DNA fragmentation secondary to ortho-coumaric acid alkyl esters

In this experiment, 200,000 GBM cells per well were seeded on a Matrigel base layer in a 24-well plate, in triplicate. After 72 h of incubation, we added BOC and IOC at 200 μM; MOC, POC, and EOC at 300 μM; and TMZ at 600 μM. After 6 or 12 h of incubation, the samples were

washed with TrypLE Express (Gibco, catalogue no. 12604013); DNA was subsequently extracted with the QIAamp kit (Qiagen, catalogue no. 51304), and quantified via spectrophotometry under ultraviolet/visible light (Thermo Scientific NanoDrop 2000). Subsequently, 500 ng/μL of DNA were homogenised and run in agarose gel at 1.8% with SYBR Safe (1 μL/10 mL) (Invitrogen, catalogue no. S33102) at 100 V for 30–45 min, and viewed in a transilluminator with photo documentation function.

Statistical analysis

Data on phosphatidylserine externalisation and on cell viability from the 3D cell culture were compared to those from the monolayer culture. We conducted a one-way analysis of variance. Cell viability data from the OCAAE experiments were compared with two-way analysis of variance. We used the post-hoc Tukey test to make intergroup comparisons. The significance threshold was set at $P < .05$, and data are reported as mean (standard deviation [SD]). Statistical analysis was conducted with the GraphPad Prism software, version 6 (GraphPad Software, San Diego, CA, USA).

Results

Matrigel three-dimensional and monolayer cultures

In this study, we compared both 3D cell culture models (Matrigel base layer and Matrigel-embedded cells) and the monolayer cell culture model. The greatest growth was observed in the Matrigel base layer culture (Fig. 1A), which presented more cells and better redistribution and cytohistological development; cells in this culture showed greater numbers of ramifications, characteristic of GBM cells, throughout the study (Fig. 1B, C, D, and E). The Matrigel-embedded cell culture (Fig. 1G) showed good development in the number of cells. However, cells did not show the ramifications characteristic of GBM cells during the 8 days of growth (Fig. 1H, I, J, and K). The monolayer culture (Fig. 1M) reached confluence before 8 days and cells began to detach; GBM cells showed all the cytohistological characteristics of a monolayer culture, with no neurosphere or dendritic spine formation or cell migration, as well as the other morphological characteristics shown in the photomicrographs (Fig. 1N, O, P, and Q).

The photomicrographs taken at the time the MTT assay was performed (Fig. 1F, L, and R) show that the salts were able to penetrate all cells throughout the 3D culture scaffold, and were not trapped in the Matrigel. MTT results from day 8 of growth show that 3D cell cultures presented good viability, with a greater percentage of growth than the monolayer cell culture (400% vs 200%) over the initial 5000 cells (at 6 h, with 100% viability); this difference was statistically significant ($P < .005$; Fig. 1S).

Synthesis and purification of ortho-coumaric acid alkyl esters

The OCAAEs evaluated in this study were obtained by chemical synthesis with Fischer esterification. The alcohols used were selected to evaluate the effect of alkyl chain elongation on the biological activity of the compounds. Thus, alkyl chain length ranged from 1 to 4 carbons, in the following order: MOC, EOC, POC, BOC/IOC. Furthermore, we used an isomer with 4 carbons (isobutanol) in order to evaluate the effect of this molecule's geometry, with greater steric hindrance in the alkyl chain, on biological activity (Fig. 2A). Alkyl chain elongation not only affects the

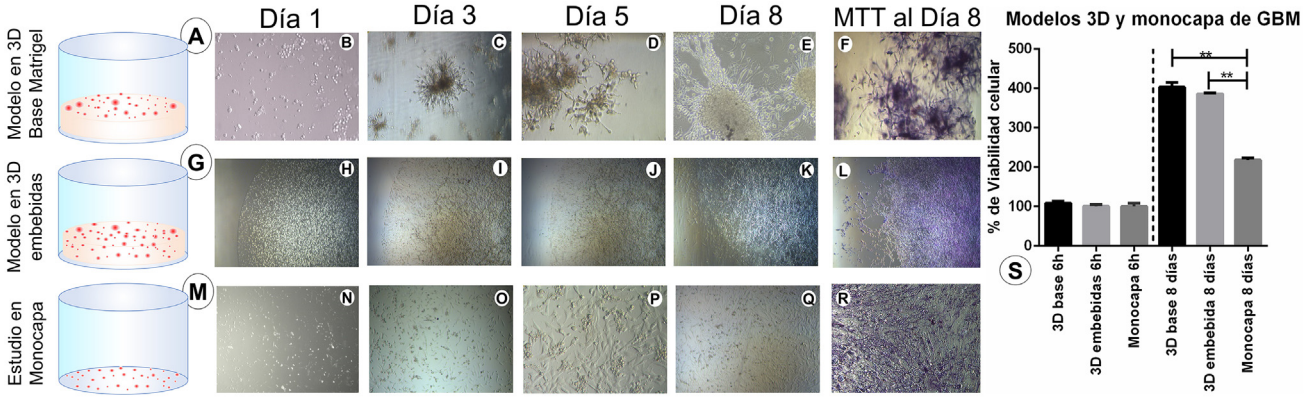

Fig. 1 Cell culture models: Three-dimensional (3D) and monolayer cultures of glioblastoma multiforme (GBM) cells, with 5000 cells/well on a 96-well plate; cell growth was monitored for 8 days. A) 3D Matrigel base layer culture of GBM cells. B–E) Photomicrographs of the 3D Matrigel base layer culture at different stages of development, with cells visible on the surface. F) MTT results on day 8. G) 3D Matrigel-embedded culture of GBM cells. H–K) Photomicrographs of the 3D Matrigel-embedded cell culture. L) MTT results on day 8. M) Monolayer cell culture. N–Q) Photomicrographs of the monolayer cell culture. R) MTT results on day 8. Images D, E, F, P, and R are shown at 20× magnification; the remaining images are shown at 10× magnification. S) Chart showing the percentage of viable cells at 8 days for the different GBM cell cultures (3D Matrigel base layer and Matrigel-embedded cell cultures, and monolayer cell culture) compared to the initial number of cells (5000 per well at 6 h). The 6-h cultures represent the number of cells used at the beginning of the study; the percentage of growth in each culture was compared after 8 days. Data are expressed as mean (SD) with differences significant at $P < .005$ (one-way ANOVA) versus the control group.

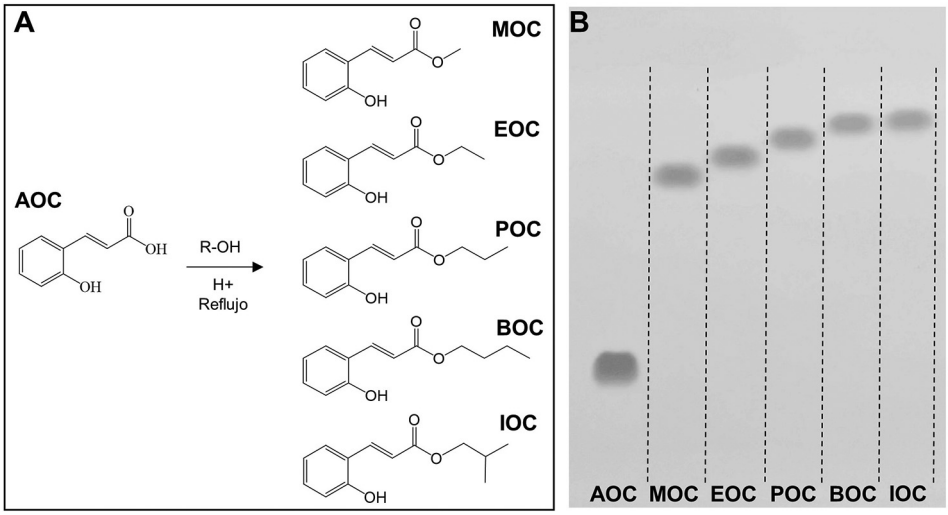

Fig. 2 Alkyl esters obtained by esterification of ortho-coumaric acid by Fischer synthesis. A) Molecular structure of the ortho-coumaric acid alkyl esters synthesised for the study. R = methyl, ethyl, propyl, butyl and isobutyl. B) Thin-layer chromatography visualisation of o-coumaric acid (AOC or OCA) and its alkyl esters: methyl-o-coumarate (MOC), ethyl-o-coumarate (EOC), propyl-o-coumarate (POC), butyl-o-coumarate (BOC), and isobutyl-o-coumarate (IOC). Visualisation under ultraviolet light (254 nm).

size and weight of the molecule, but also its octanol–water partition coefficient (logP), and therefore its capacity to penetrate lipid membranes and spread across different tissues.

The purification process produced high-purity compounds (Fig. 2B); AOC (or OCA) and its alkyl esters were able to migrate long distances due to the difference in polarity between molecules. We analysed the relative migration of the different compounds, finding the following retention factors: AOC: 0.22; MOC: 0.62; EOC: 0.67; POC: 0.71; BOC: 0.73; IOC: 0.75. AOC is the most polar molecule, and therefore presents the least migration.[25]

Evaluation of cell viability

The results on cell viability showed the cytotoxic effect of OCAAEs at different concentrations and exposure times. Cytotoxicity was more pronounced in the monolayer culture than in the 3D Matrigel base layer culture (Fig. 3, panels A1, A2, C1–C4). Table 1 shows all mean (SD) values for cell viability; for example, the monolayer culture with BOC at 100 μM presented a cell viability value of 64% (1.2), as compared to 73.3% (1.3) for the 3D culture ($P < .005$). BOC and IOC showed a higher degree of cytotoxicity than MOC, POC, and EOC, in both the monolayer and the 3D cultures ($P < .005$). However, in comparison to TMZ, all OCAAEs significantly reduced cell viability ($P < .001$). Likewise, all OCAAEs showed a considerable difference when compared to the control condition ($P > .0001$; Fig. 3, panels A1 and A2; Table 1).

In the experiments aiming to find the optimal exposure time and response, no significant differences were observed after 3 h of exposure, for any study molecule at any concentration (Fig. 3, panel B1). At 6 h of exposure to OCAAE at 300 or 500 μM, cells presented 85%–90% viability (ie, cytotoxicity of 10%–15%); this difference was significant with respect to the control condition ($P < .005$; Table 1; Fig. 3, panel B2). At 12 h of exposure (Fig. 3, panel B2), most compounds started to show a much greater effect with respect to the control group ($P < .001$ and $P < .0001$), particularly at concentrations of 300 and 500 μM, with cytotoxicity of 25%–35% (viability of 65%–75%); the experiment with TMZ continued not to present significant differences (Table 1).

At 24 h of exposure, the 3D culture (Fig. 3, panel A2) showed that, for all OCAAEs, the minimum concentration needed to observe a significant effect was 100 μM, and a concentration of 1200 μM is highly cytotoxic ($P < .0001$), whereas TMZ only presented 40% cytotoxicity (60% cell viability); OCAAEs reached their mean level of cytotoxicity at a concentration of 200–500 μM (Table 1).

Effect of combining ortho-coumaric acid alkyl esters and temozolomide

The experiment studying the combination of OCAAEs and TMZ at different concentrations found that administration of TMZ only (600 μM) was associated with cell viability of 86.0% (2.6) ($P < .05$ against the control condition), whereas the combination of TMZ plus OCAAEs was associated with a considerable decrease in cell viability: 31% (1.53) for BOC + TMZ (200/600 μM), 34% (2.33) for IOC + TMZ (200/600 μM) ($P < .0001$), 63% (1.21) for MOC + TMZ (300/600 μM), 66% (0.3) for POC + TMZ (300/600 μM), and 51% (1.45) for EOC + TMZ (300/600 μM) ($P < .0001$; Fig. 3, panel D1; Table 1). Results for OCAAEs plus TMZ at 1200 μM are not reported, as all absorbance values were close to zero (complete cytotoxicity).

Induction of apoptotic cell death secondary to ortho-coumaric acid alkyl esters

Detection of phosphatidylserine externalisation secondary to ortho-coumaric acid alkyl esters

This experiment showed that 3 h of exposure to OCAAEs promoted binding of annexin V to externalised

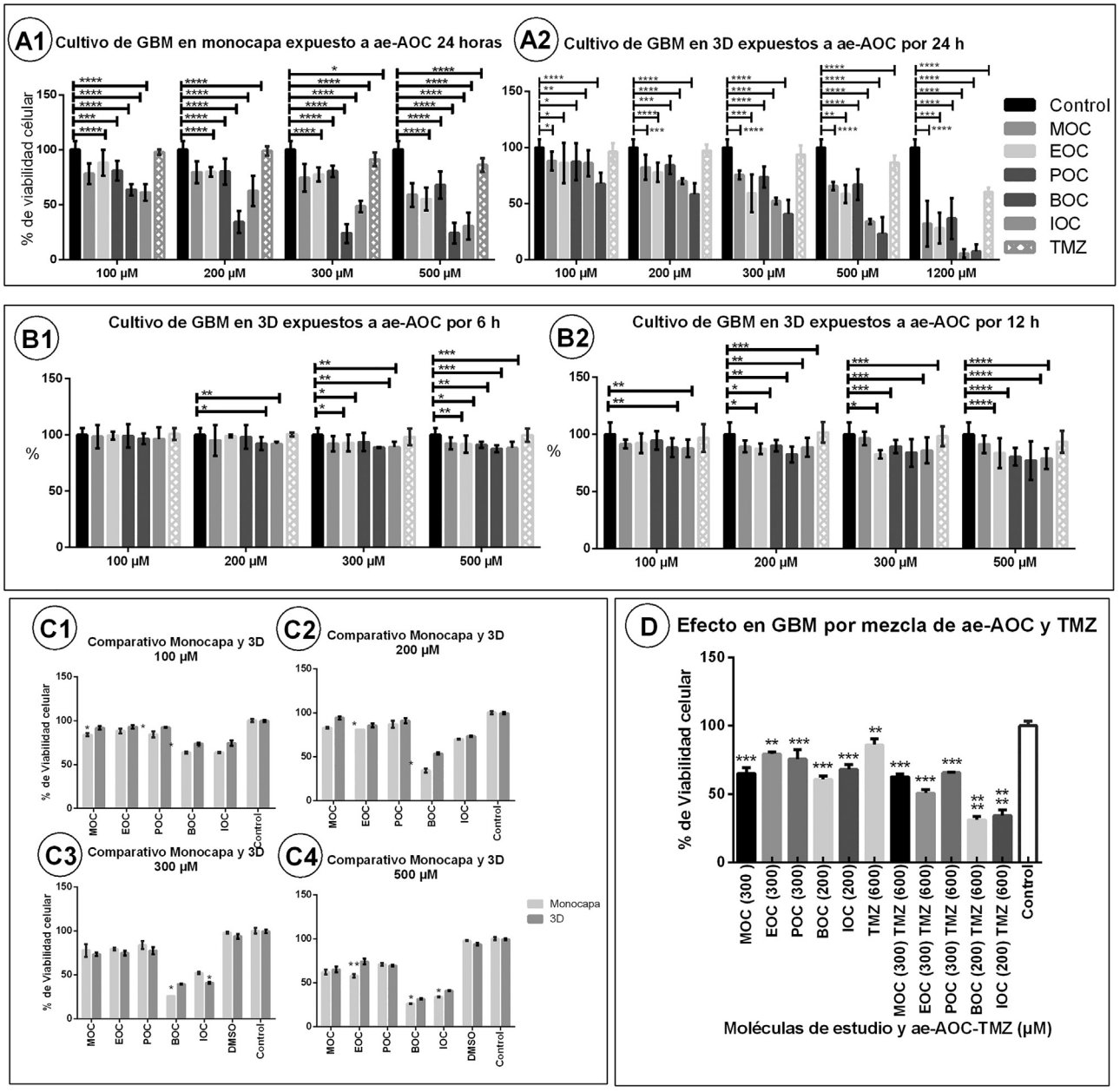

Fig. 3 Charts of mean glioblastoma multiforme (GBM) cell viability after exposure to ortho-coumaric acid alkyl esters (OCAAE). Charts show the mean (SD) percentage of viable cells according to MTT results for different doses of OCAAEs, with temozolomide as a positive control, compared to the control condition (negative stimulus). A1) Monolayer GBM cell culture at 24 h of exposure. A2) 3D Matrigel base layer culture. B1 and B2) 3D culture with 3 and 6 h of exposure, respectively. C1–C4) Comparison of the monolayer and 3D cultures after 24 h' exposure to OCAAEs at the different concentrations used. D) Percentage of viable cells after 24 h' exposure to OCAAE plus temozolomide. Results are expressed as means (SD), evaluated with the two-way ANOVA and post-hoc Tukey test. * $P < .05$, ** $P < .005$, *** $P < .001$, **** $P < .0001$.

phosphatidylserine; the percentage of cells positive for this labelling was as follows: 43.6% (0.33) for cells exposed to MOC, 67.0% (2.8) for EOC, 42.6% (0.33) for POC, 52.6% (3.7) for BOC, and 34.0% (8.08) for TMZ; all differences were significant at $P < .0001$ versus the control condition (0.18% [0.1]) (Fig. 4, panels A1–A7). However, the percentage of annexin V-positive cells decreased at 6 h of exposure: 19.3% (2.4) for MOC, 24.6% (2.02) for EOC, 17.3% (2.8) for POC, 24.3% (0.1) for BOC, and 14.6% (1.76) for TMZ; all differences were significant at $P < .005$ versus the control condition (4.66% [0.88]) (Fig. 4, panel A7).

Effect of ortho-coumaric acid alkyl esters on the expression of active caspase-3 in glioblastoma multiforme cells

Photomicrographs showing labelling of caspase-3 with Alexa-Fluor 488 (green) (Fig. 4, panels B1–B6) show the difference with respect to unlabelled cells, which only present DAPI labelling of the nucleus (blue). The mean

Table 1 Mean percentage of viable cells after exposure to ortho-coumaric acid alkyl esters at different concentrations, alone or in combination with temozolomide, with different exposure times.

Monolayer culture, 24 h' exposure						
OCA	50 μM	100 μM	200 μM	300 μM	500 μM	1200 μM
MOC	–	84 (1.7)**	83 (0.9)**	78 (3.9)***	62 (2.7)****	–
EOC	–	88 (2.5)**	81 (0.1)**	80 (0.7)***	58 (2.1)****	–
POC	–	84 (3.5)**	87 (4.1)**	84 (2.7)**	71 (1.3)****	–
BOC	–	64 (1.2)****	34 (2.2)****	26 (0.1)****	26 (0.2)****	–
IOC	–	64 (1.9)****	70 (0.5)***	52 (0.9)****	34 (0.7)****	–
TMZ	–	98 ± 0.6	99 ± 1.1	91 (1.5)*	86 (1.5)***	–
3D Matrigel base layer culture, 24 h' incubation						
MOC	–	91 (2.2)*	94 (1.8)	74 (1.1)****	65 (3.2)****	–
EOC	–	93 (1.9)	86 (2.5)**	75 (1.7)***	75 (3.2)***	–
POC	–	92 (0.3)*	91 (3.1)*	77 (2.3)***	70 (1.1)****	–
BOC	–	73 (1.3)***	54 (1.1)****	40 (0.3)****	31 (0.7)****	–
IOC	–	74 (3.1)***	73 (1.8)***	41 (0.8)****	41 (0.6)****	–
TMZ	–	99 (0.9)	99 (1.3)	94 (2.5)	85 (1.9)***	–
3D Matrigel base layer culture, 24 h' incubation						
MOC	93 (1.0)	88 (2.1)**	82 (2.6)***	76 (0.9)***	66 (0.9)****	32 (4.7)****
EOC	91 (0.1)	86 (4.2)**	78 (2.1)***	59 (3.9)****	59 (1.9)****	28 (3.2)****
POC	93 (1.0)	87 (3.8)**	84 (1.9)**	74 (2.2)***	67 (3.2)****	37 (4.3)****
BOC	92 (3.3)	68 (2.3)****	58 (2.3)****	41 (3.1)****	23 (3.5)****	7 (1.5)****
IOC	90 (2.4)	86 (2.3)**	70 (0.6)***	52 (0.7)****	34 (0.6)****	6 (0.9)****
TMZ	100 (1.5)	96 (1.8)	97 (1.2)	94 (1.9)	87 (1.5)**	60 (0.9)****
3D Matrigel base layer culture, 12 h' incubation						
MOC	–	92 (0.9)	89 (1.2)*	97 (1.4)	91 (1.8)	–
EOC	–	92 (2.0)	87 (1.1)**	83 (0.9)**	84 (3.1)**	–
POC	–	95 (1.9)	90 (1.2)*	89 (1.3)*	81 (1.8)**	–
BOC	–	88 (1.9)**	82 (1.6)**	84 (2.8)**	77 (3.9)***	–
IOC	–	88 (1.8)**	89 (1.9)**	86 (2.6)**	79 (2.1)***	–
TMZ	–	97 (2.8)	102 (2.1)	98 (2.1)	94 (2.2)	–
3D Matrigel base layer culture, 6 h' incubation						
MOC	–	98 (2.4)	95 (3.2)	92 (1.6)*	93 (1.2)*	–
EOC	–	100 (1.2)	99 (0.3)	93 (1.7)*	92 (1.8)*	–
POC	–	99 (0.8)	98 (2.4)	94 (1.9)	91 (0.6)*	–
BOC	–	97 (1.1)	92 (1.4)*	89 (0.1)**	88 (0.7)**	–
IOC	–	96 (2.4)	92 (0.5)*	89 (1.1)**	88 (1.3)**	–
TMZ	–	101 (1.1)	100 (0.4)	98 (1.7)	100 (1.3)	–
3D Matrigel base layer culture, 3 h' incubation						
MOC	–	100 (0.9)	99 (1.5)	99 (1.1)	96 (3.4)	–
EOC	–	99 (0.6)	97 (1.9)	97 (1.3)	98 (3.8)	–
POC	–	97 (2.5)	96 (1.1)	99 (2.3)	99 (1.1)	–
BOC	–	97 (1.0)	97 (0.6)	95 (2.8)	95 (2.8)	–
IOC	–	99 (1.7)	94 (2.8)	97 (1.1)	100 (0.6)	–
TMZ	–	100 (1.2)	100 (2.9)	100 (3.1)	101 (1.1)	–
3D culture exposed to OCA + TMZ						
MOC (300 μM)		65 (2.52)***	MOC (300 μM) + TMZ (600 μM)			63 (1.21)****
EOC (300 μM)		79 (0.88)***	EOC (300 μM) + TMZ (600 μM)			51 (1.45)****
POC (300 μM)		76 (3.93)***	POC (300 μM) + TMZ (600 μM)			66 (0.30)***
BOC (200 μM)		61 (1.45)***	BOC (200 μM) + TMZ (600 μM)			31 (1.53)***
IOC (200 μM)		68 (2.08)***	IOC (200 μM) + TMZ (600 μM)			34 (2.33)*****
TMZ (600 μM)		86 (2.65)**				

Values are expressed as mean (SD). Differences with the control condition are significant at *$P < .05$, **$P < .005$, ***$P < .001$, or ****$P < .0001$.

Mean percentage of viable cells according to MTT results. BOC: butyl-o-coumarate; EOC: ethyl-o-coumarate; IOC: isobutyl-o-coumarate; MOC: methyl-o-coumarate; POC: propyl-o-coumarate; TMZ: temozolomide.

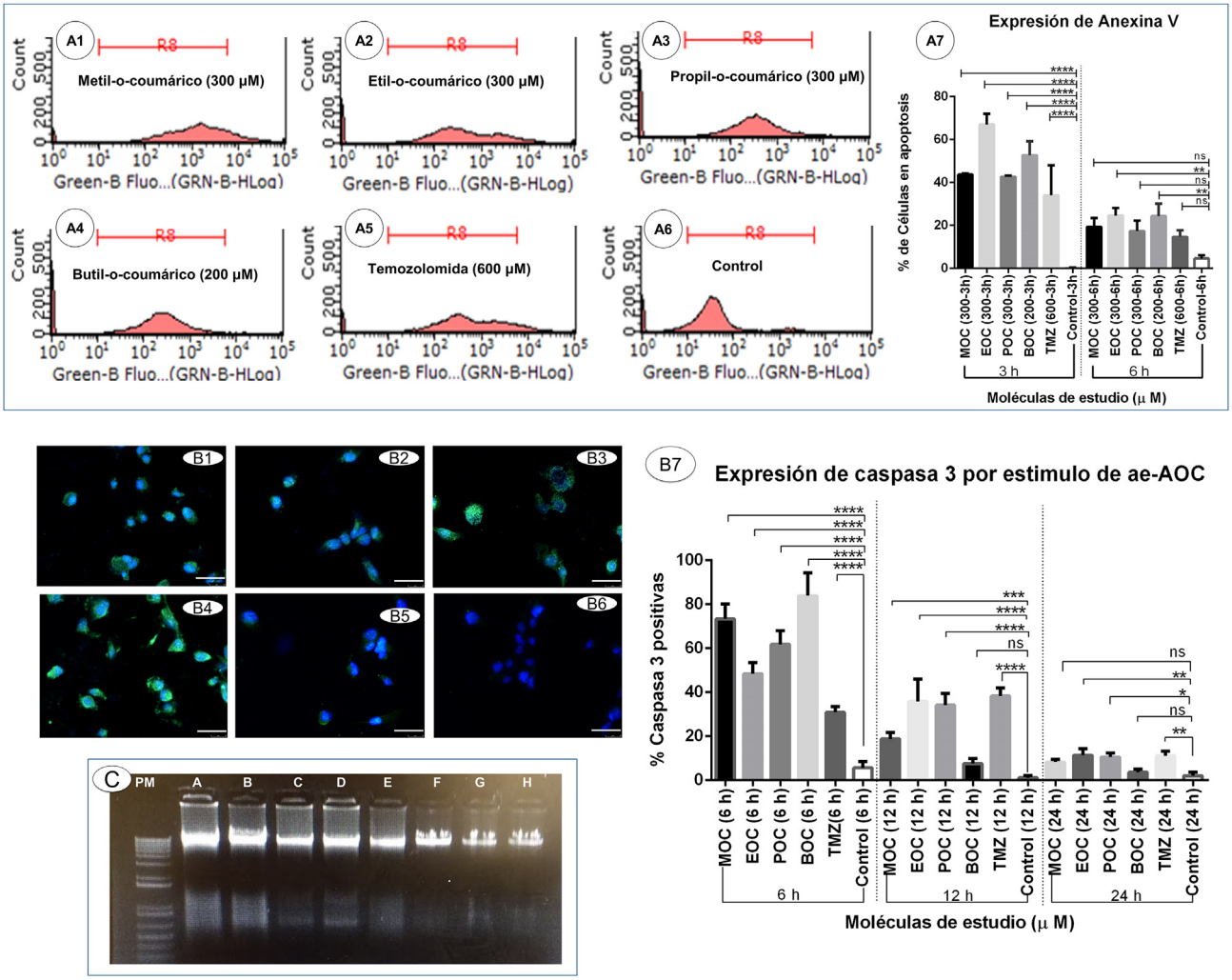

Fig. 4 Induction of apoptotic cell death secondary to ortho-coumaric acid alkyl esters (OCCAE). A1–A6) Results of flow cytometry testing for annexin V and propidium iodide to detect apoptosis in the monolayer culture of glioblastoma multiforme (GBM) cells exposed for 6 h to the study compounds. A7) Percentage of cells positive for annexin V in the different study groups in triplicate, at 3 and 6 h of exposure. Data are expressed as mean (SD) with differences significant at ***P < .001 and ****P < .0001 versus the control group. B1–B6) Expression of active caspase-3 secondary to OCAAE exposure. Immunofluorescence labelling of active caspase-3 (green) in the 3D culture of GBM cells exposed to OCAAE for 6 h. DAPI labelling of cell nuclei (blue). B1: MOC (300 µM); B2: EOC (300 µM); B3: POC (300 µM); B4: BOC (200 µM); B5: TMZ (600 µM); B6: control. Images shown at 40× magnification; scale bar measures 50 µm. B7) Percentage of cells expressing caspase-3 in a total of 30 fields counted in each group. Data are expressed as mean (SD) with differences significant at ***P < .001 and ****P < .0001 versus the control group. C) DNA ladder study in agarose gel to detect cell death after 12 h' exposure to OCAAEs. MW: molecular weight in base pairs. A: BOC (200 µM); B: IOC (200 µM); C: MOC (300 µM); D: POC (300 µM); E: EOC (300 µM); F: TMZ (600 µM); G: vehicle (DMSO); H: control (culture medium). (For interpretation of the references to colour in this figure legend, the reader is referred to the web version of this article.)

percentage of cells positive for caspase-3 after 6 h of exposure was as follows: 73.4% (3.9) for cells exposed to MOC, 48.4% (2.9) for EOC, 61.8% (3.5) for POC, 83.9% (6.08) for BOC, and 30.9% (1.52) for TMZ; all differences were significant at P < .0001 or P < .001 versus the control condition (5.6% [1.6]) (Fig. 4, panel B7). After 12 h of exposure, expression of active caspase-3 was reduced for several of the study molecules: 18.8% (1.6) for MOC, 35.8% (5.8) for EOC, 34.1% (3.03) for POC, 7.5% (1.3) for BOC, and 38.3% (2.1) for TMZ; the difference as compared to the control condition (1.1% [0.57]; P < .005) was smaller than at 6 h' exposure. At 24 h of exposure, expression of active caspase-3 was less marked for most study molecules: 3.6% (0.82) for MOC, 11.4% (1.7) for EOC, 8.2% (0.76) for POC, 1.1% (0.5) for BOC, and 11.1% (1.16) for TMZ; differences were significant at P < .05 versus the control condition (2.0% [0.94]) (Fig. 4, panel B7).

DNA fragmentation secondary to ortho-coumaric acid alkyl esters

Significant DNA fragmentation was observed after 12 h of exposure to BOC and IOC (Fig. 4, panel C: A and B). Degraded DNA was observed to a lesser extent in cells exposed to MOC, POC, and EOC (Fig. 4, panel C: C, D, and E), and was not

observed in the TMZ, vehicle, or control conditions (Fig. 4, panel C: F, G, and H). DNA degradation was not observed at 6 h of exposure.

Discussion

In this study, we evaluated the effects of the synthesised OCAAEs on the GBM cell line, and compared them against the effects of TMZ, the first-line drug for these tumours. We observed a significant reduction in cell viability after exposure to OCAAEs with longer alkyl chains, BOC, and IOC (4 carbons); however, MOC, POC, and EOC, with shorter chains (1, 2, and 3 carbons, respectively), also had significant effects at lower concentrations than TMZ, both in monolayer and 3D cultures (Fig. 3).

The fact that greater cytotoxicity was observed in the monolayer culture than in the 3D culture may be explained by the similarity between the characteristics of cells in the latter model and in *in vivo* conditions, as a result of which the cells may present greater resistance to the compounds and drugs and greater survival. They may even express a greater quantity of proteins enabling them to imitate the natural environment of the tumour, from adhesion molecules that promote invasion and metastasis to molecules promoting the survival of cancer cells, or extracellular matrix proteins that promote intercellular bonds; this would maintain their more active state.[23,24] Photomicrography images show that cells in 3D cultures presented more pronounced growth, both in number and the form of ramification, by which cells communicate and extend cytoplasmic processes to establish contact between neurospheres. These properties were not observed in the monolayer culture (Fig. 1).[26] In contrast, the Matrigel-embedded cell culture did not show clear cytohistological characteristics, possibly due to the pressure of the extracellular matrix, which may have been somewhat higher with this technique. However, cells in this culture presented good growth in terms of volume and ramifications; despite this, we opted to continue using the first 3D culture. Both monolayer and 3D cultures presented cell viability of approximately 50% with OCAAEs at low concentrations (BOC and IOC at 200 μM; MOC, POC, and EOC at 300 μM), compared to 60% viability for cells exposed to TMZ (1200 μM) (Fig. 3).[13]

We repeated the experiment for OCAAE exposure at 24 h to establish which concentrations had the greatest effect on cell viability, ranging from 50 to 1200 μM. At 50 μM, no significant differences were observed for any of the study molecules, and at 100 μM only BOC and IOC had an effect on cell viability, though limited ($P < .05$). On the other hand, concentrations of 1200 μM were highly cytotoxic for all OCAAEs. However, TMZ only reduced cell viability by 40%; therefore, much lower doses are required for OCAAEs than for TMZ in order to observe an effect on cell viability.

MTT studies of cell viability after different exposure times found no significant differences with respect to the control condition after 3 h (Table 1), whereas the experiments with annexin V found that BOC, MOC, POC, and EOC did induce apoptosis after 3 h of exposure; exposure to the latter was also associated with greater phosphatidylserine externalisation (Fig. 4, panels A1–A7). Cell viability decreased after 6 h of exposure, particularly at concentrations of 300 and 500 μM; at these low concentrations, TMZ continued not to present an effect on cell viability. While the percentage of labelled cells was much lower at 6 than at 3 h, there continued to be a significant difference with respect to the control condition (Fig. 4, panel A7), probably because some cells were at a more advanced stage of apoptosis, when phosphatyldiserine is no longer detectable, or may have entered cell-cycle arrest.[11,12,27] Similarly, active caspase-3 expression was observed in a large number of cells exposed to OCAAEs and TMZ, with significantly higher percentages at 6 h for BOC, MOC, POC, and EOC (in decreasing order of significance), compared to cells exposed to TMZ only and to the control conditions (Fig. 4, panels B1–B7); after 12 and 24 h of exposure to OCAAEs, active caspase-3 expression was lower, possibly due to advanced cell death or cell-cycle arrest.[28] The gel run technique to quantify DNA fragmentation also showed that, at 12 h of exposure, numerous cells were in a late stage of apoptosis (Fig. 4C); this is consistent with our results for other techniques studying cell death.

Other researchers who have studied the effects of hydroxycinnamic acids similar to OCA and their alkyl esters on different tumours concur that the apoptotic pathway may be activated: these studies have observed activation of such proapoptotic genes as *bax*/*bak* and *p53*, JNK proteins, caspases (3, 6, 7, and 9), Apaf-1, FasL, TRAIL-TNF, p21, p16, and Bh3-only proteins.[10,29,30] Similarly, other researchers report silencing of *Bcl-2*, ERK 1/2, cyclin D1, interaction with second messengers, and inhibition of nucleus translocation and cyclin-dependent kinases 4 and 6, modification of the retinoblastoma protein–E2F complex, cell-cycle arrest, and cell death by apoptosis; while these molecular changes may also have occurred in our experiments, we did not analyse molecules that may have confirmed this hypothesis.[28,31–33]

The combination of OCAAEs and TMZ had a greater effect on the viability of GBM cells (Fig. 3D), suggesting that very low doses of OCAAEs may be combined with TMZ to potentiate the drug's antitumour effect.[34]

OCAs occur naturally in various types of foods; however, attempts to use them therapeutically have not controlled doses or monitored effects, as they contain different phenolic compounds; on the other hand, if OCAAEs are synthesised, we are able to control the type and stability of molecules, enabling these compounds to be used at controlled doses. Furthermore, our laboratory synthesises different hydroxycinnamic acid esters using enzymatic techniques with yields superior to 95%, a more environmentally friendly and economical alternative.[18]

OCAs present low liposolubility, reducing their bioavailability and antitumour efficacy; on the other hand, OCAAEs, and particularly those with longer alkyl chains, are more liposoluble and therefore better able to penetrate membranes and act on cells, for example in cell organelles. However, their effects on healthy cells were not tested; this would require vectorisation of the compound to make it more selective to cancer cells, perhaps through the administration of nanoparticles or nanovectors such as liposomes alongside OCAAEs, which would increase their liposolubility and distribution.[35] Other possible approaches are direct administration at the time of tumour dissection,

or smart delivery by binding the OCAAE to a monoclonal antibody able to identify cancer cell epitopes; this would enable localised antitumour action.[36] However, such vectorisation may not be completely necessary, as previous studies with different hydroxycinnamic acid alkyl esters, including certain long-chain alkyl esters of p-coumaric acid, have shown low cytotoxicity in non-cancerous cell lines[28]; the same effect may be observed for the molecules synthesised in our study.[28]

Conclusions

In most of the parameters evaluated in this study, BOC and its isomer IOC presented a significantly greater effect than the other OCAAE; this may indicate a direct relationship between alkyl chain length and the reduction in GBM cell viability, with alkyl length conferring different physicochemical properties to the molecules, such as increased liposolubility. However, modifying the molecular geometry of the butyl ester did not increase the activity of the molecule. Nonetheless, our results suggest that all OCAAEs had antitumour activity, with butyl esters (BOC and IOC) presenting the greatest potential; this opens the door to further structure–function studies and research with other OCA derivatives.

These findings are consistent with those of previous studies using other types of hydroxycinnamic acids. The effects of OCAAEs mainly affect the viability of tumour cells, inducing processes associated with apoptosis; these molecules also present a synergistic effect, with their cytotoxicity being increased when administered in combination with TMZ. Furthermore, we observed a more significant effect with BOC and its isomer in several of the parameters studied, followed by MOC, POC, and EOC, whereas much higher concentrations of TMZ were needed before the same effects were observed. We also corroborated that 3D cell cultures constitute an appropriate model for studying new molecules with potential therapeutic effects in different types of tumour.

Author contributions

Yanet Karina Gutiérrez Mercado and Alejandro Arturo Canales Aguirre: study conception and design.

Juan Carlos Mateos Díaz and Doddy Denise Ojeda Hernández: synthesis of molecules.

Francisco Javier López González, Edwin Estefan Reza Zaldívar, and Mercedes Azucena Hernández Sapiens: drafting and critical review of the article.

Ulises Alfonso Gómez Pinedo: data analysis and interpretation.

Rachel Sarabia Estrada: methodology and data acquisition.

Monserrat Macías Carballo: statistical analysis.

Conflicts of interest

The authors have no financial or commercial relationships that could create conflicts of interest with regard to this article.

Acknowledgements

This study has received funding from the CONACyT post-doctoral grant awarded to Yanet Karina Gutiérrez Mercado and a grant from the Mixed Fund for Science and Technology of the State of Jalisco (grant no. JAL-2014-0-250508).

Appendix A. Supplementary data

Supplementary data to this article can be found online at https://doi.org/10.1016/j.neurop.2021.09.006.

References

1. Ostrom QT, Patil N, Cioffi G, Waite K, Kruchko C, Barnholtz-Sloan JS. CBTRUS statistical report: primary brain and other central nervous system tumors diagnosed in the United States in 2013–2017. Neuro Oncol. 2020;22(12 Suppl 2):iv1–96.
2. Friedman HS, Kerby T, Calvert H. Temozolomide and treatment of malignant glioma. Clin Cancer Res. 2000;6(7):2585–97.
3. Zhang HZ, Li CY, Wu JQ, Wang RX, Wei P, Liu MH, et al. Anti-angiogenic activity of para-coumaric acid methyl ester on HUVECs in vitro and zebrafish in vivo. Phytomedicine. 2018;48:10–20.
4. Huang B, Zhang H, Gu L, Ye B, Jian Z, Stary C, et al. Advances in immunotherapy for glioblastoma multiforme. J Immunol Res. 2017;2017:3597613.
5. Wick W, Gorlia T, Bendszus M, Taphoorn M, Sahm F, Harting I, et al. Lomustine and bevacizumab in progressive glioblastoma. N Engl J Med. 2017;377(20):1954–63.
6. Chen TC, Chuang JY, Ko CY, Kao TJ, Yang PY, Yu CH, et al. AR ubiquitination induced by the curcumin analog suppresses growth of temozolomide-resistant glioblastoma through disrupting GPX4-mediated redox homeostasis. Redox Biol. 2020;30:101413.
7. Jiapaer S, Furuta T, Tanaka S, Kitabayashi T, Nakada M. Potential strategies overcoming the temozolomide resistance for glioblastoma. Neurol Med Chir (Tokyo). 2018;58(10):405–21.
8. Pawlowska E, Szczepanska J, Szatkowska M, Blasiak J. An interplay between senescence, apoptosis and autophagy in glioblastoma multiforme-role in pathogenesis and therapeutic perspective. Int J Mol Sci. 2018;19(3).
9. Dull AM, Moga MA, Dimienescu OG, Sechel G, Burtea V, Anastasiu CV. Therapeutic approaches of resveratrol on endometriosis via anti-inflammatory and anti-angiogenic pathways. Molecules. 2019;24(4).
10. Yang GW, Jiang JS, Lu WQ. Ferulic acid exerts anti-angiogenic and anti-tumor activity by targeting fibroblast growth factor receptor 1-mediated angiogenesis. Int J Mol Sci. 2015;16(10):24011–31.
11. Kumnerdkhonkaen P, Saenglee S, Asgar MA, Senawong G, Khongsukwiwat K, Senawong T. Antiproliferative activities and phenolic acid content of water and ethanolic extracts of the powdered formula of *Houttuynia cordata* Thunb. fermented broth and *Phyllanthus emblica* Linn. fruit. BMC Complement Altern Med. 2018;18(1):130.
12. Tsai Tsai NM, Chang KF, Wang JC. Juniperus communis extract exerts antitumor effects in human glioblastomas through blood-brain barrier. Cell Physiol Biochem. 2018;49(6):2443–62.
13. Zhang X, Ni Q, Wang Y, Fan H, Li Y. Synergistic anticancer effects of formononetin and temozolomide on glioma C6 cells. Biol Pharm Bull. 2018;41(8):1194–202.
14. Ferreira PS, Victorelli FD, Fonseca-Santos B, Chorilli M. A review of analytical methods for p-coumaric acid in plant-based

products, beverages, and biological matrices. Crit Rev Anal Chem. 2019;49(1):21–31.
15. Varela MT, Ferrarini M, Mercaldi VG, Sufi BDS, Padovani G, Nazato LIS, et al. Coumaric acid derivatives as tyrosinase inhibitors: efficacy studies through in silico, in vitro and ex vivo approaches. Bioorg Chem. 2020;103:104108.
16. Baqueiro-Pena I, Contreras-Jacquez V, Kirchmayr MR, Mateos-Diaz JC, Valenzuela-Soto EM, Asaff-Torres A. Isolation and characterization of a new ferulic-acid-biotransforming bacillus megaterium from maize alkaline wastewater (Nejayote). Curr Microbiol. 2019;76(10):1215–24.
17. Contreras-Jacquez V, Rodriguez-Gonzalez J, Mateos-Diaz JC, Valenzuela-Soto EM, Asaff-Torres A. Differential activation of ferulic acid catabolic pathways of *Amycolatopsis* sp. ATCC 39116 in submerged and surface cultures. Appl Biochem Biotechnol. 2020;192(2):494–516.
18. Grajales-Hernandez DA, Armendariz-Ruiz MA, Gallego FL, Mateos-Diaz JC. Approaches for the enzymatic synthesis of alkyl hydroxycinnamates and applications thereof. Appl Microbiol Biotechnol. 2021;105(10):3901–17.
19. Obregon-Mendoza MA, Estevez-Carmona MM, Hernandez-Ortega S, Soriano-Garcia M, Ramirez-Apan MT, Orea L, et al. Retro-curcuminoids as mimics of dehydrozingerone and curcumin: synthesis, NMR, X-ray, and cytotoxic activity. Molecules. 2016;22(1).
20. Wu YJ, Su TR, Chang CI, Chen CR, Hung KF, Liu C. (+)-Bornyl p-coumarate extracted from stem of *Piper betle* induced apoptosis and autophagy in melanoma cells. Int J Mol Sci. 2020;21(10).
21. Sen A, Atmaca P, Terzioglu G, Arslan S. Anticarcinogenic effect and carcinogenic potential of the dietary phenolic acid: o-coumaric acid. Nat Prod Commun. 2013;8(9):1269–74.
22. Prestwich GD. Evaluating drug efficacy and toxicology in three dimensions: using synthetic extracellular matrices in drug discovery. Acc Chem Res. 2008;41(1):139–48.
23. Gomez-Roman N, Stevenson K, Gilmour L, Hamilton G, Chalmers AJ. A novel 3D human glioblastoma cell culture system for modeling drug and radiation responses. Neuro Oncol. 2017;19 (2):229–41.
24. Jo Y, Choi N, Kim HN, Choi J. Probing characteristics of cancer cells cultured on engineered platforms simulating different microenvironments. Artif Cells Nanomed Biotechnol. 2018;46 (sup1):1170–9.
25. Dickson H, Kittredge KW, Sarquis AM. Thin-layer chromatography: the "eyes" of the organic chemist. J Chem Educ. 2004;81 (7):1023.
26. Musah-Eroje A, Watson S. A novel 3D in vitro model of glioblastoma reveals resistance to temozolomide which was potentiated by hypoxia. J Neurooncol. 2019;142(2):231–40.
27. Singh AK, Bishayee A, Pandey AK. Targeting histone deacetylases with natural and synthetic agents: an emerging anticancer strategy. Nutrients. 2018;10(6).
28. Menezes J, Edraki N, Kamat SP, Khoshneviszadeh M, Kayani Z, Mirzaei HH, et al. Long chain alkyl esters of hydroxycinnamic acids as promising anticancer agents: selective induction of apoptosis in cancer cells. J Agric Food Chem. 2017;65(33): 7228–39.
29. Kim EY, Ryu JH, Kim AK. CAPE promotes TRAIL-induced apoptosis through the upregulation of TRAIL receptors via activation of p38 and suppression of JNK in SK-Hep1 hepatocellular carcinoma cells. Int J Oncol. 2013;43(4):1291–300.
30. Lin WL, Liang WH, Lee YJ, Chuang SK, Tseng TH. Antitumor progression potential of caffeic acid phenethyl ester involving p75(NTR) in C6 glioma cells. Chem Biol Interact. 2010;188(3): 607–15.
31. Eroglu C, Secme M, Bagci G, Dodurga Y. Assessment of the anticancer mechanism of ferulic acid via cell cycle and apoptotic pathways in human prostate cancer cell lines. Tumour Biol. 2015;36(12):9437–46.
32. Janicke B, Hegardt C, Krogh M, Onning G, Akesson B, Cirenajwis HM, et al. The antiproliferative effect of dietary fiber phenolic compounds ferulic acid and p-coumaric acid on the cell cycle of Caco-2 cells. Nutr Cancer. 2011;63(4):611–22.
33. Puangpraphant S, Berhow MA, Vermillion K, Potts G, Gonzalez de Mejia E. Dicaffeoylquinic acids in Yerba mate (Ilex paraguariensis St. Hilaire) inhibit NF-kappaB nucleus translocation in macrophages and induce apoptosis by activating caspases-8 and -3 in human colon cancer cells. Mol Nutr Food Res. 2011;55(10):1509–22.
34. Hwang TW, Kim DH, Kim DB, Jang TW, Kim GH, Moon M, et al. Synergistic anticancer effect of acteoside and temozolomide-based glioblastoma chemotherapy. Int J Mol Med. 2019;43(3): 1478–86.
35. Figueiro F, Bernardi A, Frozza RL, Terroso T, Zanotto-Filho A, Jandrey EH, et al. Resveratrol-loaded lipid-core nanocapsules treatment reduces in vitro and in vivo glioma growth. J Biomed Nanotechnol. 2013;9(3):516–26.
36. Boskovitz A, Wikstrand CJ, Kuan CT, Zalutsky MR, Reardon DA, Bigner DD. Monoclonal antibodies for brain tumour treatment. Expert Opin Biol Ther. 2004;4(9):1453–71.